HHS Public Access

Author manuscript

J Neurochem. Author manuscript; available in PMC 2017 April 20.

Published in final edited form as:

J Neurochem. 2016 February ; 136(3): 510–525. doi:10.1111/jnc.13391.

Epothilone D Prevents Binge Methamphetamine-Mediated Loss of Striatal Dopaminergic Markers

Bryan A. Killinger and **Anna Moszczynska**

Abstract

Exposure to binge methamphetamine (METH) can result in a permanent or transient loss of dopaminergic (DAergic) markers such as dopamine (DA), dopamine transporter (DAT), and tyrosine hydroxylase (TH) in the striatum. We hypothesized that the METH-induced loss of striatal DAergic markers was, in part, due to destabilization of microtubules (MTs) in the nigrostriatal DA pathway that ultimately impedes anterograde axonal transport of these markers. To test this hypothesis, adult male Sprague Dawley rats were treated with binge METH or saline in the presence or absence of epothilone D (EpoD), a MT-stabilizing compound, and assessed for the levels of several DAergic markers as well as for the levels of tubulins and their posttranslational modifications (PMTs) at 3 days after the treatments. Binge METH induced a loss of stable long-lived MTs within the striatum but not within the SNpc. Treatment with a low dose of EpoD increased the levels of markers of stable MTs and prevented METH-mediated deficits in several DAergic markers in the striatum. By contrast, administration of a high dose of EpoD appeared to destabilize MTs and potentiated the METH-induced deficits in several DAergic markers. The low-dose EpoD also prevented the METH-induced increase in striatal DA turnover and increased behavioral stereotypy during METH treatment. Together, these results demonstrate that MT dynamics plays a role in the development of METH-induced losses of several DAergic markers in the striatum and may mediate METH-induced degeneration of terminals in the nigrostriatal DA pathway. Our study also demonstrates that MT-stabilizing drugs, such as EpoD have a potential to serve as useful therapeutic agents to restore function of DAergic nerve terminals following METH exposure when administered at low doses.

Graphical abstract

Corresponding author, Anna Moszczynska, PhD, Department of Pharmaceutical Sciences, Eugene Applebaum College of Pharmacy and Health Sciences, Wayne State University, 459 Mack Ave, Detroit MI 48201, Fax: (313) 577-2033, Phone: (313) 577-1257, ei2744@wayne.edu, Designed studies, analyzed data, and edited manuscript. Bryan Andrew Killinger, M.A., Department of Pharmaceutical Sciences, Eugene Applebaum College of Pharmacy and Health Sciences, Wayne State University, 459 Mack Ave, Detroit MI 48201, Designed studies, conducted research, analyzed data, and edited manuscript.

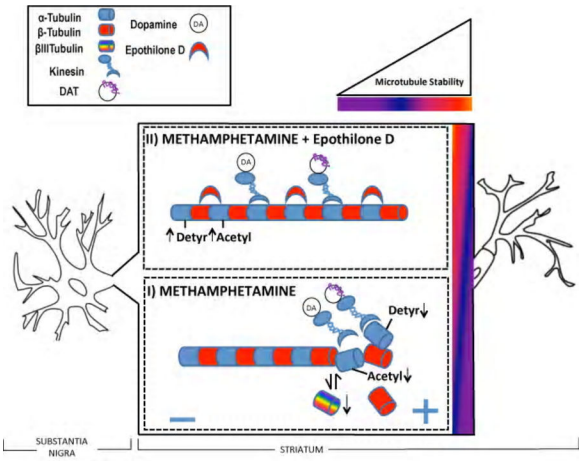

Administration of binge methamphetamine (METH) negatively impacts neurotransmission in the nigrostriatal dopamine (DA) system. The effects of METH include decreasing the levels of DAergic markers in the striatum. We have determined that high-dose METH destabilizes microtubules in this pathway, which is manifested by decreased levels of acetylated (Acetyl) and detyrosinated (Detyr) α-tubulin. A microtubule stabilizing agent epothilone D protects striatal microtubules form METH. These findings provide a new strategy for protection form METH - restoration of proper axonal transport.

Keywords

methamphetamine neurotoxicity; axonal transport; microtubules; epothilone

Background

Methamphetamine (METH) is a widely abused neurotoxic psychostimulant. When administered in high doses, METH induces long-term deficits in striatal dopaminergic (DAergic) markers, including the dopamine transporter (DAT), tyrosine hydroxylase (TH), dopamine (DA), and DA metabolites (Wagner *et al.* 1980, Preston *et al.* 1985, Harvey *et al.* 2000, Mooney *et al.* 1994). To some extent, the loss of DAT, TH, DA and its metabolites is due to a physical loss of axons (Bowyer & Schmued 2006). However, extended abstinence from METH results in recovery of these DAergic markers in experimental animals and humans (Harvey et al. 2000, Cass & Manning 1999, Friedman *et al.* 1998, Volkow *et al.* 2001, Bowyer *et al.* 1992, Volkow *et al.* 2015), suggesting compensatory changes within the nigrostriatal DA pathway. There is little evidence that DAT and TH are locally synthesized in the axons in the adult brain, and therefore, axonal transport might be required to restore DAT and TH to DAergic terminals. Axonal transport impairment is an early marker of several neurodegenerative diseases (Morfini *et al.* 2009) and may also precede development of METH neurotoxicity or play a role in predisposing METH users to development of Parkinson's disease (Callaghan *et al.* 2012). It is not known whether METH alters axonal transport in the nigrostriatal DA pathway.

Axonal transport requires cytosolic polymers called microtubules (MTs) that consist of heterodimers of the cytoskeletal proteins α-tubulin and β-tubulin. Several post-translational modifications (PTMs) of α-tubulin including detyrosination, tyrosination, and acetylation are thought to play a role in regulating MT structure and function (Wloga & Gaertig 2010). Specifically, acetylated (AcetTUB) and detyrosinated (DetyTUB) α-tubulin are highly enriched in stable long-lived MTs (Schulze *et al.* 1987), are present in axons (Brown *et al.* 1993), and preferentially recruit the anterograde motor protein kinesin (Reed *et al.* 2006, Konishi & Setou 2009). Conversely, β-tubulin (βIIITUB) imparts dynamicity to MTs (Tischfield *et al.* 2010), is highly expressed in somatic neurons (Guo *et al.* 2011), and confers resistance to taxane-mediated MT stabilization (Narvi *et al.* 2013, Hari *et al.* 2003). In axons, tyrosinated α-tubulin (TyrTUB) is enriched in newly formed MTs and in a highly dynamic MT population that is sensitive to nocodazole-mediated depolymerization (Baas & Black 1990). Overall, MTs enriched with DetyTUB and/or AcetTUB are more rigid and support axonal transport, whereas MTs enriched with TyrTUB and/or βIIITUB are more dynamic and impede axonal transport. Although early alterations in MT structure and function have been reported in several models of DA neuron neurodegeneration (Ren *et al.* 2015, Cartelli *et al.* 2013, Lu *et al.* 2014), it is not known whether neurotoxic METH treatment alters MTs in the nigrostriatal DA pathway.

Epothilone D (EpoD) is a neuroprotective taxane-like compound that stabilizes MTs, promotes MT assembly, and ultimately enhances axonal transport in neurons (Zhang *et al.* 2012). Treatment with EpoD increases the number of stable MTs that are highly enriched with AcetTUB (Fan *et al.* 2014, Brunden *et al.* 2011). Recently, it was shown that systemic injection of EpoD treatment could attenuate 1-methyl-4-phenyl-1,2,3,6-tetrahydropyridine (MPTP)-induced DAergic neuron loss in the nigrostriatal DA pathway of mice through stabilization of MTs and subsequent promotion of axonal transport (Cartelli *et al.* 2013). It is currently unknown whether EpoD treatment can prevent METH-induced deficits in striatal DAergic markers.

The primary objective of the present study was to investigate whether axonal transport plays a role in the development of deficits in DAergic markers in nigrostriatal DA axons in response to binge METH. We hypothesized that METH treatment would destabilize MTs in striatal DAergic axons, which would subsequently impair axonal transport from the SNpc to the dorsal striatum. To investigate this hypothesis, we employed a moderately toxic METH regimen to avoid extensive damage to DAergic axons and examined striatal MTs at a time point when they are expected to be maximally destabilized (Cartelli et al. 2013). To assess MT stability, we utilized antibodies against specific PTMs of α-tubulin and antibody against βIIITUB. Using immunofluorescent staining we identified a significant decrease in acetylated tubulin (AcetTUB), a marker of stable MTs, in TH-positive striatal axons in rats treated with binge METH. Our second objective was to investigate the effects of the MT-stabilizing compound EpoD on the development of METH-induced DAergic deficits and MT dynamics within the striatum. We hypothesized that EpoD treatment would prevent the METH-induced loss of striatal DAergic markers. To test this hypothesis we administered two treatment regimens of EpoD alone or in combination with binge METH to animals. The low dose of EpoD prevented decreases in the levels of DA, TH, and DAT and in the levels of AcetTUB in the striatum. The high dose of EpoD potentiated METH-induced deficits in DA,

DA metabolites and DAT and METH-induced acetylation of striatal MTs. In conclusion, our data suggest that binge METH has destabilizing effect on axonal transport in the nigrostriatal DA axons, which can be prevented by low doses of MT-stabilizing drug EpoD but not by high doses of this epothilone.

Methods and Materials

Subjects

A total of 71 adult male Sprague-Dawley rats (Harlan, Indianapolis, IN) weighing 350–400 g (on postnatal day 80) were used for experiments. All animal procedures were conducted in strict adherence to the Wayne State University Institutional Animal Care and Use Committee approved protocol # A-05–07–13.

Drug Treatments

D-Methamphetamine HCl (Sigma-Aldrich, St. Louis, MO) was dissolved in isotonic sterile saline (0.09% NaCl) to a final concentration of 10 mg/mL. Binge METH treatment consisted of 4 successive intraperitoneal (i.p.) injections of METH (10 mg/kg METH-HCl, 8 mg/kg freebase METH) administered at 2-h intervals at ambient temperature of 21–22°C. In our hands, this METH regimen leads to moderate deficits in DA (20 – 25%) when measured at 7 days after the administration of the drug (Supplementary Figure 1).

EpoD (Abcam, Cambridge, UK) was dissolved in dimethylsulfoxide (DMSO) to a final concentration of 0.5 mg/mL (working solution for low doses) and 5 mg/mL (working solution for high doses). Rats in the EpoD groups were treated with either low doses of EpoD (EpoDL) or high doses of EpoD (EpoDH). Specifically, the EpoDL group received a single injection of 0.3 mg/kg EpoD 30 min prior to METH or saline, 0.1 mg/kg during METH or saline binge (1 h after the 3rd injection), and 0.1 mg/kg 24 h after the last injection of METH or saline. The EpoDH group received a single injection of 3 mg/kg EpoD prior to METH or saline, 1 mg/kg during METH or saline treatment, and 1 mg/kg after the last injection of METH or saline. All of the rats received less than 0.4 mL/kg DMSO. Animal exposure to DMSO was minimized to avoid the potentially confounding, known side effects of DMSO (Cavaletti *et al.* 2000, Altland *et al.* 1966, Preston et al. 1985, Kleindienst *et al.* 2006, Robinson & Engelborghs 1982). Rectal temperatures were measured using a Thermotemp rectal probe (Physitemp, Clifton, NJ). All the rats were euthanized via live decapitation 3 days after the last METH or saline injection. The details of the overall study design are summarized in Figure 1. The 3rd-day time point was chosen for brain analysis because a previous study on axonal transport impairment showed that MPTP-induced changes to MTs occurred early (i.e. within 3 days) after the neurotoxic insult and *prior* to DAergic axon loss (Cartelli et al. 2013). In rats, binge METH toxicity, manifested by deficits in DAergic markers, develops over approximately 3 days (Bowyer et al. 1992, Bowyer *et al.* 1994, Cass *et al.* 2000).

Tissue Collection

All tissues were collected on ice, and the brains were rinsed with ice-cold PBS. To measure total protein and neurotransmitter levels, both the striatum and SNpc were dissected from the

right hemisphere using blunt dissection methods. The resulting tissue pieces were then immediately placed on dry ice and stored at −80°C until assayed. The left hemisphere was post-fixed in paraformaldehyde (PFA) for 72 h at 4°C. The postfixed brains were processed as previously described (Liu *et al.* 2013).

Western Blot

Western blot analysis was conducted as previously described (Liu *et al.* 2013). PVDF membranes were probed with one of the following primary antibodies: anti-DAT (Santa Cruz Biotechnology, 1:500), anti-β-actin (Cell Signaling, 1:5000), anti-DetyTUB (Millipore, 1:1000), anti-TyrTUB (Millipore, 1:1000), anti-AcetTUB (Cell Signaling, 1:1000), anti-βIIITUB (Abcam, 1:1000), anti-α-tubulin (Santa Cruz Biotechnology,1:1000), anti-dynein (Santa Cruz Biotechnology, 1:1000), anti-kinesin heavy chain (Santa Cruz, Biotechnology, 1:1000), anti-GFAP (abcam, 1:1000), anti-caspase-3 (Cell Signaling, 1:1000), or anti-4-hydroxynonenal (4-HNE (1:500, R&D Systems) and appropriate secondary antibodies. The blots were developed using a LAS4000 Bioimager (GE Healthcare, Piscataway, NJ). All the blots contained at least two samples representative of each experimental condition. Immunoreactivity was quantified using ImageJ software (National Institutes of Health, Bethesda, MD).

Immunohistochemistry

Fixed brain tissues were processed as previously described (Liu et al. 2013). Citrate buffer antigen retrieval (ThermoFisher) was applied to all tissue sections. The sections were incubated overnight at 4°C with an anti-TH antibody and antibodies specific for one of the following: AcetTUB, TyrTUB, DetyTUB, βIIITUB, or α-tubulin—all of which were diluted 1:500 in the blocking buffer. The sections were then incubated for 2.5 h at room temperature with the blocking buffer containing diluted (1:400) Alexa Fluor® 488 goat anti-mouse (Invitrogen, Carlsbad, CA) and Alexa Fluor 598 goat anti-rabbit (Invitrogen) antibody. DRAQ5 (Invitrogen) was used to stain nuclei. The sections were then mounted using Fluoromount mounting medium (Southern Biotech, Birmingham, AL). The immunostaining was imaged using the Leica SP3 laser scanning confocal microscope (Leica, Wetzlar, Germany). Non-compressed raw single z-plane images were exported from the Leica Image Analysis Suite (Leica). These images were then analyzed using Imaris co-localization analysis software (Bitplane South Windsor, CT). For each image automatic thresholding and masking functions were used to prevent interference from signal noise and variations in signal intensity. The resulting percent co-occurrence in the TH channel was normalized to that in the non-treated control for ease of graphical comparison. The final value represents the percentage of signal overlap within the TH signal.

High-Performance Liquid Chromatography

The procedures were conducted as previously described (Killinger *et al.* 2014). All the procedures were conducted on ice or under refrigeration. Briefly, the tissues were sonicated in 0.5 mL of 0.3 N perchloric acid for 30 s, and the resulting homogenate was centrifuged for 30 min at 12,000 × *g*. The pellet was dissolved in 1M NaOH overnight at 4°C, and protein concentrations were determined using the bicinchoninic acid (BCA) protein assay (ThermoScientific). To measure DA content, 20 μl of the supernatant was injected into the

mobile phase containing 90 mM sodium dihydrogen phosphate monohydrate, 50 mM citric acid, 1.7 mM 1-octane sulfonic acid, 50 μM EDTA, and 10% acetonitrile (ThermoScientific), at a flow rate of 0.5 mL/min. The samples were separated using a C-18 reverse-phase column (150 × 3.2, 3 μM particle size; ThermoScientific). DA and its metabolites were then detected electrochemically (electrode 1: −150 V, electrode 2: +220 V). The final values are reported as nanograms of analyte per microgram of protein.

Open-field Motor Activity Measurements

The gross motor activity of all the animals was assessed using the Opto-Varimex 4 Auto Track open-field Plexiglass chamber (Columbus Instruments, Columbus, OH). At the beginning of each session, the animals were placed in the middle of the Plexiglass chamber, and their subsequent movement and position were recorded continuously. For each animal, gross motor activity was assessed for three 30-min sessions. The sessions were conducted the day before METH treatment, immediately after the third METH injection (before the 2nd EpoD dose), and 24 h after the last METH injection (before the 3rd EpoD dose). Locomotor activity was calculated automatically from the raw beam-break data by the Opto-Varimex software.

Statistical Analysis

Data sets containing two experimental groups were analyzed using unpaired two-tailed Student's *t*-tests, with Bonferroni correction when applicable. To analyze data sets with 3 or more groups, one-way analysis of variance (ANOVA) followed by Tukey's *post hoc* test was performed. Two-way ANOVA was performed on selected data sets to determine whether there was an interaction between METH and EpoD effects. Two-way repeated measures ANOVA with Student-Newman-Keuls *post hoc* test was used to analyze the core body temperature data. Immunofluorescence co-occurrence was calculated using Leica Software Suite (Leica). Acclimation behavior was analyzed using simple linear regression analysis. All graphs were generated using GraphPad Prism 5 (GraphPad Software Inc., La Jolla, CA), and all statistical operations were performed using SPSS (IBM). Statistical significance was set at $p<0.05$.

Results

The Effect of Binge METH on DAergic Markers in the Striatum

Prior to the treatments, the average core body temperature of the animals was 36.6°C, which is a normal temperature for adult male rats (Figure 2A). Saline treatment did not significantly affect core body temperature at any time point. One hour after the first injection of METH, the rats had an average temperature of 38.9°C. The core body temperatures of the METH-treated animals significantly increased at 1, 3, 5, and 7 h after the first METH injection compared to saline controls. Core body temperatures were the highest at 5 h and 7 h after the first METH injection, with mean values of 39.8°C and 40.5°C, respectively.

Compared to striatal whole-tissue lysates from saline-treated rats, there were significant reductions in both DAT (−68%) and TH (−33%) immunoreactivity in striatal whole-tissue lysates from METH-treated animals at 3 days after the last injection of the drug (Figure 2B,

D). There was no significant difference in DAT and TH immunoreactivity between saline and METH rats in the SNpc tissue lysates (Figure 2C). The loss of striatal DAT and TH was verified in fluorescently labeled brain slices, which showed a visible and proportional reduction in DAT and TH signal within the striatum of the METH-treated rats compared with the striatum of the saline controls (Figure 2E). High-contrast single plane images of TH-labeled striatal axons in the striatum showed swollen axons and fragmented TH immunoreactivity 3 days after METH (Figure 2F).

The Effect of Binge METH on Microtubules in the Nigrostriatal Dopamine Pathway

AcetTUB, DetyTUB, TyrTUB, and βIIITUB immunoreactivities were detectable in both the SNpc and the striatum (Figure 3A). There were no detectable differences in the immunoreactivity of any of the tubulins in the SNpc tissue lysates between the saline- and METH-treated rats (Figure 3B). The immunoreactivity of both βIIITUB and DetyTUB was significantly lower (−10% and −14%, respectively) in the striatal lysates of the METH-treated animals compared to the lysates of the saline-treated controls (Figure 3C). AcetTUB and TyrTUB immunoreactivity in striatal lysates did not differ between saline- and METH-treated animals. The ratio of TyrTUB to DetyTUB was significantly higher (+26%) in striatal lysates of animals treated with METH than in saline controls (Figure 3D).

Because MT PTMs that are assessed in total tissue lysates are not specific for DAergic axons, we probed striatal tissue sections with anti-TH antibody and antibodies against different tubulins to assess METH effect on MTs in DAergic axons. The results showed high basal levels of DetyTUB, AcetTUB, and βIIITUB in the striatum (Figure 3F, G, and H). In agreement with previous reports, these MT populations were differentially expressed in axons and cell bodies; more specifically, DetyTUB and AcetTUB were more enriched in axons as opposed to the cell bodies. DetyTUB, AcetTUB, and βIIITUB were highly expressed in DAergic axons as well as in the surrounding TH-negative axons and cell bodies (Figure 3F, G, and H). In the rats treated with METH, DAergic axons were enriched with βIIITUB (Figure 3H) and deficient in both AcetTUB (Figure 3F) and DetyTUB (Figure 3G). The immunofluorescence co-occurrence analysis revealed a significant loss in AcetTUB in the TH-positive axons (−52%) 3 days after binge METH as compared to saline controls (Figure 3E). There was a loss of DetyTUB immunoreactivity that did not reach statistical significance (−33%). TyrTUB was not readily detectable in the TH-positive axons and, therefore, not quantified (data not shown).

The Effect of EpoD on METH-induced Alterations to Microtubules in the Striatum

Treatment with EpoDL slightly increased DetyTUB immunoreactivity in the striatum following saline (+36%) and markedly following METH (+78%) when compared to DMSO/saline treatment (Figure 4A). When compared to EpoDL/saline, DetyTUB increased in EpoDL/METH group by 31%. Treatment with EpoDH had little effect on the tubulins when administered alone, but when EpoDH was administered with METH, it resulted in a substantial loss of DetyTUB signal compared to DMSO/saline (−60%) and EpoDH/saline (−63%) group. All treatments minimally affected total striatal TyrTUB immunoreactivity. Compared to DMSO/saline, AcetTUB levels were reduced in the animals treated with both DMSO/METH and EpoDH/METH (−36% and −70%, respectively). Compared to EpoDH/

saline, EpoDH/METH decreased AcetTUB levels by 67%). By contrast, the animals treated with EpoDL had AcetTUB levels similar to those treated with DMSO/saline and those treated with EpoDL/saline. The animals treated with DMSO/METH and EpoDH/METH had significantly lower levels of striatal βIIITUB compared with the DMSO/saline-treated animals (−46% and −55%, respectively) (Figure 4B). α-Tubulin levels were similar across all the treatment groups. The animals treated with METH exhibited a significant loss of the motor protein dynein (−28%) (Figure 4C). By contrast, the animals treated with EpoDL and EpoDH together with METH did not show the loss of dynein in the striatum. Striatal kinesin signal was significantly greater in the striatal lysates of animals treated with EpoDH/METH (162%), but unchanged in all other treatment groups. EpoDL decreased the ratio of TyrTUB to DetyTUB in the striatum when administered with METH treatment (−70%) (Figure 4D). The animals treated with EpoDH/METH showed a 2.8-fold increase in the ratio of TyTUB to DetyTUB than animals treated with EpoDL/METH.

The core body temperature profiles for the rats used in this experiment (Figures 4–6) are shown in Figure 6A. The average core body temperature (36.8°C) remained unchanged at all time points after treatment with DMSO/saline, EpoDL/saline, or EpoDH/saline (Figure 6A). The animals treated with METH had significant hyperthermia at 1, 3, 5, and 7 hours after the first injection of METH as compared to saline controls. A maximum mean body temperature of 39.8°C for was observed in the DMSO/METH and EpoDH/METH group at 3 h after te first METH injection. The EpoDH/METH group reached 40.0°C 7 hours after METH. There were no significant differences in hyperthermia between DMSO/METH-, EpoDL/METH-, and EpoDH/METH-treated rats with the exception of EpoDL/METH *vs.* EpoDH/METH group comparison at 7 h after the first METH injection. Even though the maximum core body temperatures in DMSO/METH group were lower in the second than in the first experiment (39.8°C vs. 40.5° C), the deficits in DAT and TH between the experiments were not very different (−68% and −33% vs. −50% and −27%). The loss of AcetyTUB was higher while the loss of DetyTUB was lower in the second experiment (−14% vs. −36%), suggesting that the METH-induced changes in MT PMTs do not depend on temperature. In support, there was no correlation between AcetyTUB or DetyTUB and METH-induced hyperthermia (not shown).

Effect of EpoD on METH-induced Decreases in the Levels of DAergic Markers in the Striatum

Treatment with EpoDL alone increased striatal DA content by 40% without significantly affecting the levels of DA metabolites 3,4-dihydroxyphenylacetic acid (DOPAC) or homovanillic acid (HVA) (Figure 5A, B, and C). Conversely, the animals treated with EpoDH exhibited reduced striatal DA content (−50%) without reducing striatal DOPAC or HVA content. The animals treated with METH alone had lower striatal DA and DOPAC tissue concentrations (−63% and −48%, respectively) compared with the saline-treated animals. EpoDL attenuated the METH-induced deficit in DA (−43%). Similar reductions in striatal DOPAC and HVA content were found in the EpoDL-treated rats and the rats treated with METH alone. The ratio of the DOPAC to DA was similar in the animals treated with DMSO/saline, EpoDL/saline, and EpoDH/saline. Following METH, rats treated with DMSO or EpoDH showed a significant increase in the ratio of DOPAC to DA compared to the

control rats (~2- and ~3-fold, respectively); EpoDL restored DOPAC/DA ratio to the control value i.e., the animals treated with EpoDL/METH had a similar ratio of DOPAC to DA as the DMSO/saline-treated controls (Figure 5D).

Both EpoD treatments significantly increased DAT (2.3-fold and 1.6-fold, respectively) (Figure 5E), but not TH (Figure 5F), immunoreactivity in the striatal lysates. The animals treated with DMSO/METH had significant reductions in both DAT (−50%) and TH (−27%). Although there was a significant reduction in striatal DAT when comparing EpoDL/saline- and EpoDL/METH-treated rats (−55%), the EpoDL/METH-treated animals had DAT levels that were similar to those of the DMSO/saline-treated animals, indicating a “rescue” of DAT levels by EpoDL. The animals treated with EpoDH/METH showed drastic reductions in striatal DAT immunoreactivity (i.e., >80%). The loss of TH in the EpoDH/METH-treated animals was similar to that in the DMSO/METH-treated animals. Reductions in TH were not observed in the EpoDL/METH-treated animals compared to DMSO/saline. Compared to EpoDL/saline controls, EpoDL/METH treatment decreased DA, DOPAC, DAT, and TH levels to similar extents as METH treatment compared to saline treatment (by 59%, 36, 55%, and 18%, respectively). EpoDH/METH-induced decreases in relation to EpoDH/saline controls (−86%, −69%, −70%, −36%) where larger than those induced by DMSO/METH compared to DMSO/saline controls.

To assess inflammatory response in the experimental groups, GFAP immunoreactivity was measured in striatal lysates by western blotting. Compared to DMSO/saline controls, GFAP immunoreactivity was significantly increased in the striatum 3 days after DMSO/METH (+57%) and EpoDH/METH (+69%) treatment (Figure 5G). In contrast, GFAP expression was not significantly increased in the animals treated with EpoDL/METH. Although full-length pro-caspase-3 (~35 kDa) was detected in all the lysates, the activated cleaved caspase-3 (~15 kDa) was not detected in striatal lysates under any treatment condition. Striatal levels of 4-HNE were slightly increased (~10%) after binge METH alone (data not shown).

Behavioral Response of Rats Treated with Both EpoD and METH

Figure 6B–D depicts the analysis of motor activity counts 24 h before, during (after the 3rd METH injection), and 24 h after binge METH. Prior to METH administrations, the animals in all treatment groups displayed similar locomotor activity profile (Figure 6B). A similar pattern of locomotor activity was maintained across all the sessions by the animals treated with DMSO/saline and EpoDH/saline. The animals treated with EpoDL/saline displayed increased stereotypy (seen as dense green nodules) during the treatment phase. The animals treated with DMSO/METH also displayed more stereotypy than DMSO/saline controls but less than EpoDL/METH-treated rats (Figure 6C). The animals treated with EpoDH/METH displayed less stereotypy than other METH groups; instead, they maintained hyperlocomotion during METH administration. The treatment with EpoDL/METH produced the highest levels of stereotypy and the greatest suppression of distance traveled. During the post-treatment phase (24 h post-METH), the animals treated with METH showed significant reduction in the overall motor activity when compared to saline controls regardless of EpoD dose.

During the pre-treatment session, the animals from all groups displayed normal acclimation behavior that was characterized by a marked negative correlation between the distance travelled and the duration of the session (Figure 6D). The animals treated with either DMSO/saline, EpoDL/saline, or EpoDH/saline exhibited similar acclimation behavior throughout all the behavioral sessions. However, in the animals treated with DMSO/METH, EpoDL/METH, or EpoDH/METH, the slope between the distance traveled and time was lost during the treatment session due to stereotypy, with animals from the EpoDH group moving around and exhibiting stereotypy. During the post-treatment, the slope for DMSO/METH and EpoDL/METH groups recovered slightly (to 23% and 10%, respectively, of their pretreatment values).

Discussion

Our first major finding was the loss of stable MTs in striatal DAerigic axons following binge METH. Although we report the loss of a few tubulins in the striatum, only the loss of AcetTUB appeared to be specific for striatal DAergic axons. Our second significant finding was that the treatment with the MT-stabilizing drug EpoD could prevent the METH-mediated loss of AcetTUB and the loss of striatal DAergic markers when administered at a low dose while potentiating METH-mediated losses of DAergic markers and markers of stable MTs when administered at a high dose. Finally, we demonstrated that EpoD treatment produced acute effects on METH-induced hyperlocomotion and stereotypy, raising the possibility that MT stabilization has an effect on DA signaling.

Binge METH administration results in both reversible and irreversible loss of striatal DAergic markers with the latter being considered a manifestation of “classic” METH neurotoxicity. These “classic” neurotoxic effects of METH are mediated, in part, by oxidative stress (Yamamoto & Zhu 1998) and can induce reactive gliosis and pro-apoptotic caspase-3 cleavage throughout the striatum (Jayanthi *et al.* 2004, Zhu *et al.* 2005, Bowyer et al. 1994). We observed only a mild increase in the immunoreactivity of the reactive gliosis marker GFAP and no signal for cleaved caspase-3 in the striatum of METH-treated animals (Figure 5I). Striatal levels of 4-hydroxynonenal were also only slightly increased (~10%) after binge METH (data not shown). These results suggest that the METH-induced oxidative stress and loss of DAergic terminals was modest and that the marked deficits in DA, DAT and DOPAC were, in most part, reversible and caused by other than neurodegeneration mechanisms. Consequently, the MT alterations we are describing predominantly reflect combination of transient METH effects on MTs and neuroadaptive responses in DAergic neurons, and not “classic” neurotoxicity *per se* (i.e. a physical loss of DAergic axons). This interpretation is further supported by a relatively modest reduction in striatal DA content (~22%) observed 7 days following the same regimen of binge METH (Supplementary Figure 1). DA deficits are normally much greater (>60%) in “classic” METH neurotoxicity models at this time point (Bowyer *et al.* 1998, Bowyer et al. 1994). We did observe swollen axons with discontinuous TH signal in the striatum following METH; these axons were similar to the "empty" axons lacking vesicles, mitochondria, and other components detected in the nigrostriatal DA pathway in 1-methyl-4-phenylpyridinium (MPP+)-treated mice (Cartelli *et al.* 2013). Some of these TH-positive axons are likely irreversibly damaged (Bowyer & Schmued 2006), but the GFAP and TH data suggest that most axons are not. The

lack of gross neurotoxicity is likely explained by the lack of severe hyperthermia (≥41°C), which is a crucial determinant of METH-induced neurotoxicity (Bowyer et al. 1994, Bowyer et al. 1992). In our hands, the METH-treated animals displayed acute hyperthermia; however, the effect was modest (average core body temperature of approximately 40°C). Some of the effects of METH on DAergic markers at regimens that do not increase core body temperatures above 40.5°C are short-lasting (Bowyer et al. 1992, Bowyer et al. 1994, Harvey et al. 2000, Cass & Manning 1999, Friedman et al. 1998), a finding that agrees with higher DA loss at 3 days than at 7 days after METH in our drug regimen. However small, the increase in GFAP immunoreactivity was present in DMSO/METH and EpoDH/METH groups, but not in EpoDL/METH group, suggesting that administration of EpoDL with METH prevented METH-triggered reactive gliosis. Lack of caspase-3 activation in the striatum indicates that EpoDH did not augment METH-mediated toxic events such as mitochondrial dysfunction or oxidative stress in striatal neuronal cell bodies (Yamamoto *et al.* 2010).

The heterogeneity of α-tubulin PTMs in polymerized MTs is thought to impart their different functions (Janke 2014, Verhey & Gaertig 2007, Wehenkel & Janke 2014). MTs that are enriched in AcetTUB and DetyTUB preferentially recruit the anterograde motor protein kinesin and promote axonal transport (Reed et al. 2006, Liao & Gundersen 1998) whereas TyrTUB is highly enriched in newly formed and dynamic MTs (Baas & Black 1990). In agreement with recent findings in endothelial cells (Fernandes *et al.* 2015), we found that METH exposure led to the loss of AcetTUB, which is highly enriched in stable MTs. The loss of AcetTUB was more pronounced in TH-positive striatal axons than in striatal tissue lysates (Figure 3), suggesting some level of specificity of this effect for striatal DAergic axons. METH also resulted in a significant increase in the ratio of TyrTUB to DetyTUB, further suggesting the loss of stable MTs within the striatum. The increased ratio of TyrTUB to DetyTUB may also be indicative of the increased recruitment of CAP-glycine proteins (Erck *et al.* 2005, Peris *et al.* 2006), which are required for initiation of dynein-mediated retrograde axonal transport (Moughamian *et al.* 2013), possibly to remove cellular components oxidatively damaged by METH (Lin *et al.* 2012, Chevalier-Larsen & Holzbaur 2006).

The βIIITUB deficit observed in METH-treated rats could reflect decreased levels of MTs in DAergic axon (Wen *et al.* 2010). This scenario is unlikely because the co-occurrence of βIIITUB with TH immunostaining was not decreased. Alternatively, given the known MT-destabilizing effects of βIIITUB overexpression (Hari et al. 2003), the loss of striatal βIIITUB might reflect increased MT stability in non-DAergic striatal components, such as neurons, in response to METH. βIIITUB has numerous functions, including a role in mitochondrial respiration, neurogenesis, axonal guidance and intracellular trafficking as well as axonal maintenance, including association of MTs with kinesin (Roskams *et al.* 1998, Menezes & Luskin 1994, Mariani *et al.* 2015, Tischfield et al. 2010). METH-mediated alterations in any of these functions or adaptive responses to METH effects could be reflected in the βIIITUB deficit (Tulloch *et al.* 2014, Ujike *et al.* 2002, Yamamoto et al. 2010). In summary, our results suggest that METH exposure resulted in the loss of stable MTs in striatal DAergic axons, an effect that would impede axonal transport and could

account for the transient (i.e. reversible) loss of striatal DA, DOPAC, DAT, and TH observed 3 days after METH.

The loss of AcetTUB can impair axonal transport (Godena *et al.* 2014). Since EpoD increases AcetTUB levels (Fan et al. 2014, Cartelli et al. 2013), we hypothesized that EpoD would attenuate the METH-induced deficits in AcetTUB and, ultimately, the loss of striatal DAergic markers. Only the low dose of EpoD (EpoDL) produced the desired effects. EpoDL prevented the METH-mediated loss of AcetTUB (Figure 4), DA, DAT, and TH (Figure 5). As the deficits in striatal DAergic markers were similar in DMSO/METH and EpoDL/METH rats when compared to their respective controls, the EpoDL protection likely involved keeping DAergic markers at the physiological levels via axonal transport and not via attenuation of neurodegeneration. In agreement, EpoDL increased striatal DetyTUB levels and, consequently, the ratio of DetyTUB to TyrTUB while administered alone and in combination with METH, supporting also the data on a robust effect of epothilones on MT stability (Ruschel *et al.* 2015, Janke & Kneussel 2010, Cheng *et al.* 2008). In contrast, co-administration of EpoDH with METH resulted in a potentiation of the METH-induced loss of AcetyTUB and in a drastic loss of DetyTUB and DAergic markers. Lack of an effect of EpoD and METH, alone or in combination, on TyrTUB levels suggests the lack of their effect on the formation of new MTs (Janke & Kneussel 2010). Collectively, our data indicate that the low-dose EpoD stabilized MTs and restored the levels several striatal DAergic markers decreased by METH whereas high-dose EpoD impaired MT function and potentiated the depletion of striatal DA and DAT induced by METH. It was not surprising given the known neurotoxic potential of taxols (Scripture *et al.* 2006). Consequently, treatments with EpoD at doses outside the “therapeutic window” may produce unintended neuropathy in humans, particularly those with already compromised CNS such as METH users. Neuroprotective EpoD doses are likely different for different species. The high dose of EpoD was chosen based on the results from a previous study in which this dose was found to be neuroprotective against MPTP (Cartelli et al. 2013). Their study employed mice and mice differ from rats and humans in responses to DAergic toxins. In humans, recent phase 1 clinical trials testing EpoD effects against Alzheimer disease employed 10 to 1000-fold less EpoD than the dose in the investigation of Cartelli and colleagues.

The animals treated with EpoDH/METH exhibited a drastic increase in kinesin levels. Motor protein kinesin is guided from the cell body to the axon by tyrosination of α-tubulin (Konishi & Setou 2009). Therefore, the METH-induced increases in kinesin might reflect an adaptational response in moderately destabilized striatal MTs in the axons or cell bodies surrounding the striatal DAergic axons. Previous findings have suggested a role of kinesin in the initial neural plasticity and development of drug addiction (Bilecki *et al.* 2009, Tomas *et al.* 2005). METH exposure induces dendritic spines plasticity in the dorsal striatum (Jedynak *et al.* 2007). Therefore, the increase in kinesin observed in the EpoDH/METH group could be explained by an increase in dendritic plasticity in this brain area. Future studies are needed to determine the specificity and function of METH-induced kinesin upregulation.

In the striatum, DAergic innervation constitutes less than 1% of total pool of striatal components. EpoD- and METH-induced alterations in tubulin PTMs and in MT-associated proteins observed in the striatal whole-tissue lysates were 10% or greater; therefore, it is

likely that the METH-induced alterations of MTs are not exclusive to DAergic axons. Nevertheless, the METH-induced changes in particular MT PMTs within DAergic axons might be different from the changes induced by the drug within other striatal components.

EpoDL alone increased striatal DA, suggesting that EpoD increased the DA vesicle pool, possibly by promoting anterograde axonal transport of DA-containing vesicles (Franker & Hoogenraad 2013, Ren *et al.* 2005). EpoDH had the opposite effect on the striatal DA content, causing a marked reduction in the neurotransmitter. It is unclear why the two EpoD doses produced the opposite responses. Administration of high EpoD doses can result in overstabilization of MTs (Mercado-Gomez *et al.* 2004), with a consequent impairment of axonal transport (Stamer *et al.* 2002). We did not observe an increase in AcetyTUB after EpoDH alone in the striatal lysates; however, such increase might have occurred in DAergic terminals. Alternatively, EpoD may have had an effect on DA synthesis and/or metabolism (Bouvrais-Veret *et al.* 2008, Brun *et al.* 2005). As expected (Boger *et al.* 2007), METH treatment increased the ratio of DOPAC to DA. EpoDH treatment exacerbated the METH-induced increase in ratio of DOPAC to DA whereas EpoDL produced the opposite result than EpoDH, seemingly suppressing METH-induced increase in the DOPAC/DA ratio. EpoDL treatment alone had similar effect on the DAT as it had on DA levels, while striatal TH levels remained relatively unchanged (Figure 5), suggesting that EpoDL treatment preferentially enhances anterograde transport of the DAT and DA storage vesicles in relation to TH. This differential effect may be explained by differences in cargo transport rates. In general, membrane proteins are transported by fast axonal transport while cytosolic proteins primarily by slow axonal transport (Brown 2003). Consequently, the DAT could have been transported at a higher rate than TH, causing EpoD enhancement of axonal transport at the 3-days time point more obvious for the DAT than TH. On the other hand, TH, DA, and DAT all can be transported by fast axonal transport (Lechardeur *et al.* 1993, Rao *et al.* 2012) and, therefore, the observed differences might not be simply due to different axonal transport velocities. EpoD may have differentially affected retrograde axonal transport or terminal turnover (degradation) of these DAergic markers (they are degraded by different cellular processes: the proteasome, enzymatic metabolism, and lysosome, respectively). In the absence of METH, EpoDL and EpoDH both increased the levels of striatal DAT but had different effects on MT stability. Literature data indicates that both stabilization and destabilization of MTs can induce increased trafficking of the DAT to the plasma membrane (Fjorback *et al.* 2011, Herring *et al.* 2008), thus indicating the importance of proper balance in MT dynamics. In the presence of METH, EpoDH decreased the immunoreactivity of DAT. This could have resulted from METH-mediated inhibition of DAT axonal transport overcoming the effect of EpoDH.

It can be speculated that enhancing anterograde transport of DA storage vesicles and DAT would increase cytosolic DA levels within DA terminals and would exacerbate METH neurotoxicity (Yamamoto et al. 2010). In our study, EpoDL increased striatal DAT and DA levels and decreased the METH-induced loss of DAergic markers. The increase in DAT was higher than the increase in DA; this might have resulted in increased release of DA via the DAT and, consequently, prevented DA-mediated oxidative stress. Our behavioral data (Figure 6) supports this scenario. EpoDH alone also increased the striatal DAT levels, but resulted in drastic depletions of DAT and DA contents following METH. The additive DA

and DAT depleting effects of EpoDH and METH was likely a consequence of destabilization of MTs by both drugs via their depolarization (Higashi *et al.* 1989, Ruschel et al. 2015) and/or changes to DAergic markers metabolism or turnover. Finally, since binge METH impairs mitochondrial function and decreases ATP (Yamamoto et al. 2010), a deficit in ATP may have contributed to decreased transport of DAergic markers, and mitochondria, to the terminals.

METH-induced DA release induces locomotor activation and binge METH can result in long-lasting alterations in locomotor behavior (Kuczenski *et al.* 1991, Wallace *et al.* 1999). As expected, METH alone increased stereotypy during its administration and 24 h later as well as disrupted normal acclimation behavior and suppressed locomotor activity 24 h after METH exposure (Figure 6). EpoDL alone increased stereotypy during the treatment session, but had little effect on locomotor activity 24 h following treatments. This suggests there may be some acute effects of EpoD on signaling in the nigrostriatal DA pathway. The influence of MT stability on DA signaling and local DA synthesis may account for this effect (Bouvrais-Veret et al. 2008, Brun et al. 2005). These studies showed decreased DAergic neurotransmission in mice with decreased MT stability, manifested by decreased levels of DA and its metabolites, decreased DA synthesis and release, decreased levels of DA D2 receptor, and decreased locomotor activity during the day. The EpoDL-induced increase in MT stabilization evoked opposite effects with upregulation of DAT levels possibly reflecting an adaptive response to the increase in DA release. Administration of EpoDL with METH appeared to exacerbate the METH-induced effects on stereotypy, likely due to combined effect on DA release. Animals in the EpoDL/METH group displayed a nearly 2-fold increase in this measure compared to DMSO/METH-treated animals, while EpoDH suppressed METH-induced stereotypy. The dose-dependent biphasic effect of EpoD on METH-induced stereotypy during the treatment paralleled EpoDL effects on DAergic markers observed on the 3rd day. METH-induced stereotypy is mediated by postsynaptic D1 receptors in the striatum (Chartoff *et al.* 2001). Hence, the data suggests that the EpoDL-mediated changes in MTs and DAergic markers occurred during METH administration and increased DA efflux. It is plausible that the “protective” effect of EpoDL involved decreasing the levels of free intracellular DA and, consequently, preventing DA-mediated oxidative stress, a notion supported by lack of increased GFAP expression. The EpoDL protection could have also involved keeping up proper axonal transport not only of DAergic markers but also of mitochondria and removal of damaged components from DAergic terminals (Kevenaar & Hoogenraad 2015). In contrast, EpoDH-induced potentiation of METH-induced losses in DAergic markers could have been mediated by impaired anterograde transport of these markers and mitochondria, as well as by impaired removal of damaged neuronal components due to inhibition of their retrograde transport or autophagy (LaPointe *et al.* 2013, Hayashi *et al.* 2009, Castino *et al.* 2008). The emergence of hyperlocomotion instead of stereotypy in EpoDH/METH rats suggests a decrease in DAergic neurotransmission and supports the notion of an impaired transport of DA-containing vesicles. An alternative explanation for the decreased DAergic neurotransmission in these rats is EpoDH-mediated suppression of DAT activity with a resultant decrease in the reverse transport of DA and an increase in free cytosolic DA and its metabolism. This is supported by the increased DOPAC/DA ratio in EpoDH/METH rats. An increase in free DA

accompanied by a deficit in ATP (due to an impaired transport of mitochondria) could have increased an oxidative stress within DAergic terminals. All the animals displayed a significant suppression of behavior following METH regardless of EpoD dose, suggesting the changes in DAergic markers persisting at 3 days post-METH did not affect motor activities. Together, the locomotor activity data support the hypothesis that EpoD may have acute effects on striatal DAergic signaling. Future studies should focus on measuring DA release in the striatum following EpoD treatment in order to clarify molecular mechanisms underlying these findings.

In summary, we found a deficit in stable MTs, accompanying deficits in DAergic markers, within striatal DAergic axons 3 days following binge METH exposure. Furthermore, treatment with a low dose of MT-stabilizing drug EpoD prevented the METH-mediated loss of stable MTs and loss of striatal DAergic markers. The deficits in MT stability have been implicated in DA signaling-related disorders including schizophrenia, depression, and Parkinson's disease (Fournet *et al.* 2012b, Bouvrais-Veret et al. 2008, Brun et al. 2005, Morfini et al. 2009). EpoD has been tested, with some success, to treat these disorders (Fournet *et al.* 2012a, Daoust *et al.* 2014, Morfini et al. 2009). Our data suggests that EpoD may be effective in restoring striatal axonal transport and DAergic function in animal models of METH abuse (Robinson & Berridge 1993, Schultz 2007, Nutt *et al.* 2015) and also in human users of the drug, potentially attenuating the risk for development of Parkinson's disease (Callaghan et al. 2012). Further studies are needed to determine the "therapeutic window" for the treatment of METH neurotoxicity.

Supplementary Material

Refer to Web version on PubMed Central for supplementary material.

Acknowledgments

This work was supported by National Institutes of Health RO1 grant # DA034783.

Abbreviations

AcetTUB	acetylated α-tubulin
αTUB	α-tubulin
βIIITUB	βIII tubulin
BCA	bicinchoninic acid
DetyTUB	detyrosinated α-tubulin
DAergic	dopaminergic
DA	dopamine
DAT	dopamine transporter
DMSO	dimethylsulfoxide

EpoD	Epothilone D
METH	methamphetamine
MTs	microtubules
MPTP	1-methyl-4-phenyl-1,2,3,6-tetrahydropyridine
PFA	paraformaldehyde
PTMs	posttranslational modifications
SNpc	substantia nigra *pars compacta*
TH	tyrosine hydroxolase
TyrTUB	tyrosinated α-tubulin
WB	western blotting

References

Altland PD, Highman B, Parker M. Induction of hypothermia by dimethyl sulfoxide in rats exposed to cold: tissue and enzyme changes. Proc Soc Exp Biol Med. 1966; 123:853–859. [PubMed: 5959031]

Baas PW, Black MM. Individual microtubules in the axon consist of domains that differ in both composition and stability. J Cell Biol. 1990; 111:495–509. [PubMed: 2199458]

Bilecki W, Wawrzczak-Bargiela A, Przewlocki R. Regulation of kinesin light chain 1 level correlates with the development of morphine reward in the mouse brain. Eur J Neurosci. 2009; 30:1101–1110. [PubMed: 19735294]

Boger HA, Middaugh LD, Patrick KS, Ramamoorthy S, Denehy ED, Zhu H, Pacchioni AM, Granholm AC, McGinty JF. Long-term consequences of methamphetamine exposure in young adults are exacerbated in glial cell line-derived neurotrophic factor heterozygous mice. J Neurosci. 2007; 27:8816–8825. [PubMed: 17699663]

Bouvrais-Veret C, Weiss S, Hanoun N, Andrieux A, Schweitzer A, Job D, Hamon M, Giros B, Martres MP. Microtubule-associated STOP protein deletion triggers restricted changes in dopaminergic neurotransmission. J Neurochem. 2008; 104:745–756. [PubMed: 18199119]

Bowyer JF, Davies DL, Schmued L, Broening HW, Newport GD, Slikker W Jr, Holson RR. Further studies of the role of hyperthermia in methamphetamine neurotoxicity. J Pharmacol Exp Ther. 1994; 268:1571–1580. [PubMed: 8138969]

Bowyer JF, Frame LT, Clausing P, Nagamoto-Combs K, Osterhout CA, Sterling CR, Tank AW. Long-term effects of amphetamine neurotoxicity on tyrosine hydroxylase mRNA and protein in aged rats. J Pharmacol Exp Ther. 1998; 286:1074–1085. [PubMed: 9694971]

Bowyer JF, Schmued LC. Fluoro-Ruby labeling prior to an amphetamine neurotoxic insult shows a definitive massive loss of dopaminergic terminals and axons in the caudate-putamen. Brain Res. 2006; 1075:236–239. [PubMed: 16458862]

Bowyer JF, Tank AW, Newport GD, Slikker W Jr, Ali SF, Holson RR. The influence of environmental temperature on the transient effects of methamphetamine on dopamine levels and dopamine release in rat striatum. J Pharmacol Exp Ther. 1992; 260:817–824. [PubMed: 1346646]

Brown A. Axonal transport of membranous and nonmembranous cargoes: a unified perspective. J Cell Biol. 2003; 160:817–821. [PubMed: 12642609]

Brown A, Li Y, Slaughter T, Black MM. Composite microtubules of the axon: quantitative analysis of tyrosinated and acetylated tubulin along individual axonal microtubules. J Cell Sci. 1993; 104(Pt 2):339–352. [PubMed: 8505364]

Brun P, Begou M, Andrieux A, et al. Dopaminergic transmission in STOP null mice. J Neurochem. 2005; 94:63–73. [PubMed: 15953350]

Brunden KR, Yao Y, Potuzak JS, et al. The characterization of microtubule-stabilizing drugs as possible therapeutic agents for Alzheimer's disease and related tauopathies. Pharmacol Res. 2011; 63:341–351. [PubMed: 21163349]

Callaghan RC, Cunningham JK, Sykes J, Kish SJ. Increased risk of Parkinson's disease in individuals hospitalized with conditions related to the use of methamphetamine or other amphetamine-type drugs. Drug Alcohol Depend. 2012; 120:35–40. [PubMed: 21794992]

Cartelli D, Casagrande F, Busceti CL, et al. Microtubule alterations occur early in experimental parkinsonism and the microtubule stabilizer epothilone D is neuroprotective. Sci Rep. 2013; 3:1837. [PubMed: 23670541]

Cass WA, Manning MW. Recovery of presynaptic dopaminergic functioning in rats treated with neurotoxic doses of methamphetamine. J Neurosci. 1999; 19:7653–7660. [PubMed: 10460271]

Cass WA, Manning MW, Bailey SL. Restorative effects of GDNF on striatal dopamine release in rats treated with neurotoxic doses of methamphetamine. Ann N Y Acad Sci. 2000; 914:127–136. [PubMed: 11085315]

Castino R, Lazzeri G, Lenzi P, Bellio N, Follo C, Ferrucci M, Fornai F, Isidoro C. Suppression of autophagy precipitates neuronal cell death following low doses of methamphetamine. J Neurochem. 2008; 106:1426–1439. [PubMed: 18489716]

Cavaletti G, Oggioni N, Sala F, Pezzoni G, Cavalletti E, Marmiroli P, Petruccioli MG, Frattola L, Tredici G. Effect on the peripheral nervous system of systemically administered dimethylsulfoxide in the rat: a neurophysiological and pathological study. Toxicol Lett. 2000; 118:103–107. [PubMed: 11137315]

Chartoff EH, Marck BT, Matsumoto AM, Dorsa DM, Palmiter RD. Induction of stereotypy in dopamine-deficient mice requires striatal D1 receptor activation. Proc Natl Acad Sci U S A. 2001; 98:10451–10456. [PubMed: 11517332]

Cheng KL, Bradley T, Budman DR. Novel microtubule-targeting agents - the epothilones. Biologics. 2008; 2:789–811. [PubMed: 19707459]

Chevalier-Larsen E, Holzbaur EL. Axonal transport and neurodegenerative disease. Biochim Biophys Acta. 2006; 1762:1094–1108. [PubMed: 16730956]

Daoust A, Bohic S, Saoudi Y, Debacker C, Gory-Faure S, Andrieux A, Barbier EL, Deloulme JC. Neuronal transport defects of the MAP6 KO mouse - a model of schizophrenia - and alleviation by Epothilone D treatment, as observed using MEMRI. Neuroimage. 2014; 96:133–142. [PubMed: 24704457]

Erck C, Peris L, Andrieux A, et al. A vital role of tubulin-tyrosine-ligase for neuronal organization. Proc Natl Acad Sci U S A. 2005; 102:7853–7858. [PubMed: 15899979]

Fan Y, Wali G, Sutharsan R, Bellette B, Crane DI, Sue CM, Mackay-Sim A. Low dose tubulin-binding drugs rescue peroxisome trafficking deficit in patient-derived stem cells in Hereditary Spastic Paraplegia. Biol Open. 2014; 3:494–502. [PubMed: 24857849]

Fernandes S, Salta S, Summavielle T. Methamphetamine promotes alpha-tubulin deacetylation in endothelial cells: the protective role of acetyl-l-carnitine. Toxicol Lett. 2015; 234:131–138. [PubMed: 25703822]

Fjorback AW, Sundbye S, Dachsel JC, Sinning S, Wiborg O, Jensen PH. P25alpha / TPPP expression increases plasma membrane presentation of the dopamine transporter and enhances cellular sensitivity to dopamine toxicity. FEBS J. 2011; 278:493–505. [PubMed: 21182589]

Fournet V, de Lavilleon G, Schweitzer A, Giros B, Andrieux A, Martres MP. Both chronic treatments by epothilone D and fluoxetine increase the short-term memory and differentially alter the mood status of STOP/MAP6 KO mice. J Neurochem. 2012a; 123:982–996. [PubMed: 23013328]

Fournet V, Schweitzer A, Chevarin C, Deloulme JC, Hamon M, Giros B, Andrieux A, Martres MP. The deletion of STOP/MAP6 protein in mice triggers highly altered mood and impaired cognitive performances. J Neurochem. 2012b; 121:99–114. [PubMed: 22146001]

Franker MA, Hoogenraad CC. Microtubule-based transport - basic mechanisms, traffic rules and role in neurological pathogenesis. J Cell Sci. 2013; 126:2319–2329. [PubMed: 23729742]

Friedman SD, Castaneda E, Hodge GK. Long-term monoamine depletion, differential recovery, and subtle behavioral impairment following methamphetamine-induced neurotoxicity. Pharmacol Biochem Behav. 1998; 61:35–44. [PubMed: 9715805]

Godena VK, Brookes-Hocking N, Moller A, Shaw G, Oswald M, Sancho RM, Miller CC, Whitworth AJ, De Vos KJ. Increasing microtubule acetylation rescues axonal transport and locomotor deficits caused by LRRK2 Roc-COR domain mutations. Nat Commun. 2014; 5:5245. [PubMed: 25316291]

Guo J, Qiang M, Luduena RF. The distribution of beta-tubulin isotypes in cultured neurons from embryonic, newborn, and adult mouse brains. Brain Res. 2011; 1420:8–18. [PubMed: 21962533]

Hari M, Yang H, Zeng C, Canizales M, Cabral F. Expression of class III beta-tubulin reduces microtubule assembly and confers resistance to paclitaxel. Cell Motil Cytoskeleton. 2003; 56:45–56. [PubMed: 12905530]

Harvey DC, Lacan G, Tanious SP, Melega WP. Recovery from methamphetamine induced long-term nigrostriatal dopaminergic deficits without substantia nigra cell loss. Brain Res. 2000; 871:259–270. [PubMed: 10899292]

Hayashi S, Yamamoto A, You F, Yamashita K, Ikegame Y, Tawada M, Yoshimori T, Shimizu S, Nakashima S. The stent-eluting drugs sirolimus and paclitaxel suppress healing of the endothelium by induction of autophagy. Am J Pathol. 2009; 175:2226–2234. [PubMed: 19815708]

Herring NR, Schaefer TL, Gudelsky GA, Vorhees CV, Williams MT. Effect of +-methamphetamine on path integration learning, novel object recognition, and neurotoxicity in rats. Psychopharmacology (Berl). 2008; 199:637–650. [PubMed: 18509623]

Higashi H, Inanaga K, Nishi S, Uchimura N. Enhancement of dopamine actions on rat nucleus accumbens neurones in vitro after methamphetamine pre-treatment. J Physiol. 1989; 408:587–603. [PubMed: 2550628]

Janke C. The tubulin code: molecular components, readout mechanisms, and functions. J Cell Biol. 2014; 206:461–472. [PubMed: 25135932]

Janke C, Kneussel M. Tubulin post-translational modifications: encoding functions on the neuronal microtubule cytoskeleton. Trends Neurosci. 2010; 33:362–372. [PubMed: 20541813]

Jayanthi S, Deng X, Noailles PA, Ladenheim B, Cadet JL. Methamphetamine induces neuronal apoptosis via cross-talks between endoplasmic reticulum and mitochondria-dependent death cascades. FASEB J. 2004; 18:238–251. [PubMed: 14769818]

Jedynak JP, Uslaner JM, Esteban JA, Robinson TE. Methamphetamine-induced structural plasticity in the dorsal striatum. Eur J Neurosci. 2007; 25:847–853. [PubMed: 17328779]

Kevenaar JT, Hoogenraad CC. The axonal cytoskeleton: from organization to function. Front Mol Neurosci. 2015; 8:44. [PubMed: 26321907]

Killinger B, Shah M, Moszczynska A. Co-administration of betulinic acid and methamphetamine causes toxicity to dopaminergic and serotonergic nerve terminals in the striatum of late adolescent rats. J Neurochem. 2014; 128:764–775. [PubMed: 24151877]

Kleindienst A, Dunbar JG, Glisson R, Okuno K, Marmarou A. Effect of dimethyl sulfoxide on blood-brain barrier integrity following middle cerebral artery occlusion in the rat. Acta Neurochir Suppl. 2006; 96:258–262. [PubMed: 16671466]

Konishi Y, Setou M. Tubulin tyrosination navigates the kinesin-1 motor domain to axons. Nat Neurosci. 2009; 12:559–567. [PubMed: 19377471]

Kuczenski R, Segal DS, Aizenstein ML. Amphetamine, cocaine, and fencamfamine: relationship between locomotor and stereotypy response profiles and caudate and accumbens dopamine dynamics. J Neurosci. 1991; 11:2703–2712. [PubMed: 1715389]

LaPointe NE, Morfini G, Brady ST, Feinstein SC, Wilson L, Jordan MA. Effects of eribulin, vincristine, paclitaxel and ixabepilone on fast axonal transport and kinesin-1 driven microtubule gliding: implications for chemotherapy-induced peripheral neuropathy. Neurotoxicology. 2013; 37:231–239. [PubMed: 23711742]

Lechardeur D, Castel MN, Reibaud M, Scherman D, Laduron PM. Axonal transport of dopamine-containing vesicles labelled in vivo with [3H]reserpine. Eur J Neurosci. 1993; 5:449–453. [PubMed: 8261121]

Liao G, Gundersen GG. Kinesin is a candidate for cross-bridging microtubules and intermediate filaments. Selective binding of kinesin to detyrosinated tubulin and vimentin. J Biol Chem. 1998; 273:9797–9803. [PubMed: 9545318]

Lin M, Chandramani-Shivalingappa P, Jin H, Ghosh A, Anantharam V, Ali S, Kanthasamy AG, Kanthasamy A. Methamphetamine-induced neurotoxicity linked to ubiquitin-proteasome system dysfunction and autophagy-related changes that can be modulated by protein kinase C delta in dopaminergic neuronal cells. Neuroscience. 2012; 210:308–332. [PubMed: 22445524]

Liu B, Traini R, Killinger B, Schneider B, Moszczynska A. Overexpression of parkin in the rat nigrostriatal dopamine system protects against methamphetamine neurotoxicity. Exp Neurol. 2013; 247:359–372. [PubMed: 23313192]

Lu X, Kim-Han JS, Harmon S, Sakiyama-Elbert SE, O'Malley KL. The Parkinsonian mimetic, 6-OHDA, impairs axonal transport in dopaminergic axons. Mol Neurodegener. 2014; 9:17. [PubMed: 24885281]

Mariani M, Karki R, Spennato M, Pandya D, He S, Andreoli M, Fiedler P, Ferlini C. Class III beta-tubulin in normal and cancer tissues. Gene. 2015; 563:109–114. [PubMed: 25839941]

Menezes JR, Luskin MB. Expression of neuron-specific tubulin defines a novel population in the proliferative layers of the developing telencephalon. J Neurosci. 1994; 14:5399–5416. [PubMed: 8083744]

Mercado-Gomez O, Ferrera P, Arias C. Histopathologic changes induced by the microtubule-stabilizing agent Taxol in the rat hippocampus in vivo. J Neurosci Res. 2004; 78:553–562. [PubMed: 15449327]

Mooney DJ, Hansen LK, Langer R, Vacanti JP, Ingber DE. Extracellular matrix controls tubulin monomer levels in hepatocytes by regulating protein turnover. Mol Biol Cell. 1994; 5:1281–1288. [PubMed: 7696710]

Morfini GA, Burns M, Binder LI, et al. Axonal transport defects in neurodegenerative diseases. J Neurosci. 2009; 29:12776–12786. [PubMed: 19828789]

Moughamian AJ, Osborn GE, Lazarus JE, Maday S, Holzbaur EL. Ordered recruitment of dynactin to the microtubule plus-end is required for efficient initiation of retrograde axonal transport. J Neurosci. 2013; 33:13190–13203. [PubMed: 23926272]

Narvi E, Jaakkola K, Winsel S, Oetken-Lindholm C, Halonen P, Kallio L, Kallio MJ. Altered TUBB3 expression contributes to the epothilone response of mitotic cells. Br J Cancer. 2013; 108:82–90. [PubMed: 23321512]

Nutt DJ, Lingford-Hughes A, Erritzoe D, Stokes PR. The dopamine theory of addiction: 40 years of highs and lows. Nat Rev Neurosci. 2015; 16:305–312. [PubMed: 25873042]

Peris L, Thery M, Faure J, et al. Tubulin tyrosination is a major factor affecting the recruitment of CAP-Gly proteins at microtubule plus ends. J Cell Biol. 2006; 174:839–849. [PubMed: 16954346]

Preston KL, Wagner GC, Schuster CR, Seiden LS. Long-term effects of repeated methylamphetamine administration on monoamine neurons in the rhesus monkey brain. Brain Res. 1985; 338:243–248. [PubMed: 2411342]

Rao A, Richards TL, Simmons D, Zahniser NR, Sorkin A. Epitope-tagged dopamine transporter knock-in mice reveal rapid endocytic trafficking and filopodia targeting of the transporter in dopaminergic axons. FASEB J. 2012; 26:1921–1933. [PubMed: 22267337]

Reed NA, Cai D, Blasius TL, Jih GT, Meyhofer E, Gaertig J, Verhey KJ. Microtubule acetylation promotes kinesin-1 binding and transport. Curr Biol. 2006; 16:2166–2172. [PubMed: 17084703]

Ren Y, Jiang H, Hu Z, Fan K, Wang J, Janoschka S, Wang X, Ge S, Feng J. Parkin Mutations Reduce the Complexity of Neuronal Processes in iPSC-Derived Human Neurons. Stem Cells. 2015; 33:68–78. [PubMed: 25332110]

Ren Y, Liu W, Jiang H, Jiang Q, Feng J. Selective vulnerability of dopaminergic neurons to microtubule depolymerization. J Biol Chem. 2005; 280:34105–34112. [PubMed: 16091364]

Robinson J, Engelborghs Y. Tubulin polymerization in dimethyl sulfoxide. J Biol Chem. 1982; 257:5367–5371. [PubMed: 7068596]

Robinson TE, Berridge KC. The neural basis of drug craving: an incentive-sensitization theory of addiction. Brain Res Brain Res Rev. 1993; 18:247–291. [PubMed: 8401595]

Roskams AJ, Cai X, Ronnett GV. Expression of neuron-specific beta-III tubulin during olfactory neurogenesis in the embryonic and adult rat. Neuroscience. 1998; 83:191–200. [PubMed: 9466409]

Ruschel J, Hellal F, Flynn KC, et al. Axonal regeneration. Systemic administration of epothilone B promotes axon regeneration after spinal cord injury. Science. 2015; 348:347–352. [PubMed: 25765066]

Schultz W. Multiple dopamine functions at different time courses. Annu Rev Neurosci. 2007; 30:259–288. [PubMed: 17600522]

Schulze E, Asai DJ, Bulinski JC, Kirschner M. Posttranslational modification and microtubule stability. J Cell Biol. 1987; 105:2167–2177. [PubMed: 3316248]

Scripture CD, Figg WD, Sparreboom A. Peripheral neuropathy induced by paclitaxel: recent insights and future perspectives. Curr Neuropharmacol. 2006; 4:165–172. [PubMed: 18615126]

Stamer K, Vogel R, Thies E, Mandelkow E, Mandelkow EM. Tau blocks traffic of organelles, neurofilaments, and APP vesicles in neurons and enhances oxidative stress. J Cell Biol. 2002; 156:1051–1063. [PubMed: 11901170]

Tischfield MA, Baris HN, Wu C, et al. Human TUBB3 mutations perturb microtubule dynamics, kinesin interactions, and axon guidance. Cell. 2010; 140:74–87. [PubMed: 20074521]

Tomas M, Marin P, Megias L, Egea G, Renau-Piqueras J. Ethanol perturbs the secretory pathway in astrocytes. Neurobiol Dis. 2005; 20:773–784. [PubMed: 15953732]

Tulloch IK, Afanador L, Baker L, Ordonez D, Payne H, Mexhitaj I, Olivares E, Chowdhury A, Angulo JA. Methamphetamine induces low levels of neurogenesis in striatal neuron subpopulations and differential motor performance. Neurotox Res. 2014; 26:115–129. [PubMed: 24549503]

Ujike H, Takaki M, Kodama M, Kuroda S. Gene expression related to synaptogenesis, neuritogenesis, and MAP kinase in behavioral sensitization to psychostimulants. Ann N Y Acad Sci. 2002; 965:55–67. [PubMed: 12105085]

Verhey KJ, Gaertig J. The tubulin code. Cell Cycle. 2007; 6:2152–2160. [PubMed: 17786050]

Volkow ND, Chang L, Wang GJ, et al. Loss of dopamine transporters in methamphetamine abusers recovers with protracted abstinence. J Neurosci. 2001; 21:9414–9418. [PubMed: 11717374]

Volkow ND, Wang GJ, Smith L, Fowler JS, Telang F, Logan J, Tomasi D. Recovery of dopamine transporters with methamphetamine detoxification is not linked to changes in dopamine release. Neuroimage. 2015; 121:20–28. [PubMed: 26208874]

Wagner GC, Ricaurte GA, Seiden LS, Schuster CR, Miller RJ, Westley J. Long-lasting depletions of striatal dopamine and loss of dopamine uptake sites following repeated administration of methamphetamine. Brain Res. 1980; 181:151–160. [PubMed: 7350950]

Wallace TL, Gudelsky GA, Vorhees CV. Methamphetamine-induced neurotoxicity alters locomotor activity, stereotypic behavior, and stimulated dopamine release in the rat. J Neurosci. 1999; 19:9141–9148. [PubMed: 10516332]

Wehenkel A, Janke C. Towards elucidating the tubulin code. Nat Cell Biol. 2014; 16:303–305. [PubMed: 24691257]

Wen HL, Lin YT, Ting CH, Lin-Chao S, Li H, Hsieh-Li HM. Stathmin, a microtubule-destabilizing protein, is dysregulated in spinal muscular atrophy. Hum Mol Genet. 2010; 19:1766–1778. [PubMed: 20176735]

Wloga D, Gaertig J. Post-translational modifications of microtubules. J Cell Sci. 2010; 123:3447–3455. [PubMed: 20930140]

Yamamoto BK, Moszczynska A, Gudelsky GA. Amphetamine toxicities: classical and emerging mechanisms. Ann N Y Acad Sci. 2010; 1187:101–121. [PubMed: 20201848]

Yamamoto BK, Zhu W. The effects of methamphetamine on the production of free radicals and oxidative stress. J Pharmacol Exp Ther. 1998; 287:107–114. [PubMed: 9765328]

Zhang B, Carroll J, Trojanowski JQ, et al. The microtubule-stabilizing agent, epothilone D, reduces axonal dysfunction, neurotoxicity, cognitive deficits, and Alzheimer-like pathology in an interventional study with aged tau transgenic mice. J Neurosci. 2012; 32:3601–3611. [PubMed: 22423084]

Zhu JP, Xu W, Angulo JA. Disparity in the temporal appearance of methamphetamine-induced apoptosis and depletion of dopamine terminal markers in the striatum of mice. Brain Res. 2005; 1049:171–181. [PubMed: 16043139]

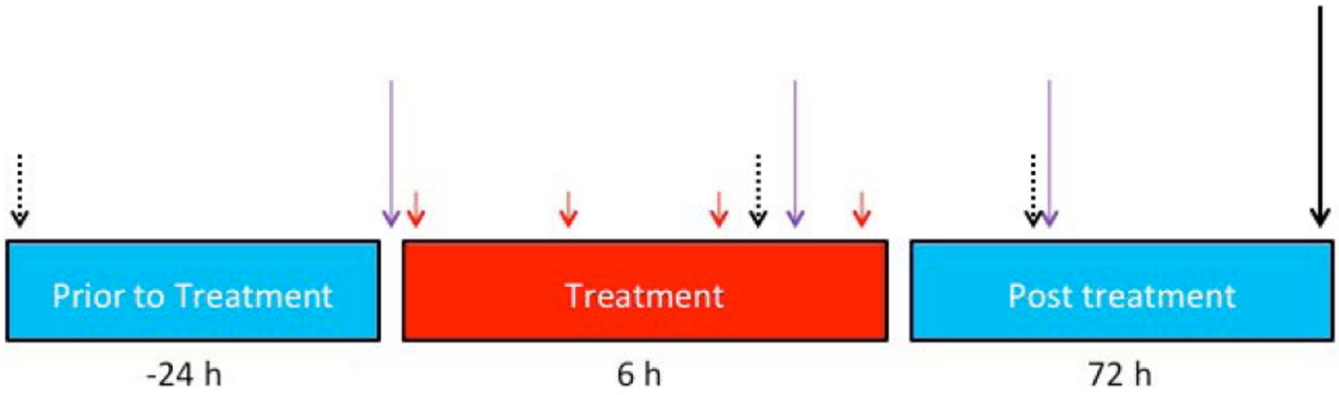

Figure 1. Study Design

Adult male Sprague-Dawley rats weighing 350–400 g were used for all experiments. Methamphetamine chloride (METH HCl) (4 × 10 mg/kg, i.p.) or saline (1 mL/kg) was administered to rats at 2-h intervals (solid red arrows). The animals were euthanized 3 days after the last METH or saline injection (solid black arrows) and assessed for the levels of tubulins and dopaminergic (DAergic) markers in the striatum and substantia nigra *pars compacta* (SNpc). A separate group of rats was treated with a microtubule-stabilizing drug epothilone D (EpoD) or vehicle 24 h before, during (after the 3rd injection) and 24 h after binge METH or saline treatment (purple arrows). Three 30-minute open-field motor activity measurements were performed for both groups at times indicated by dotted black arrows. The second group of animals was also euthanized at 3 days after the last METH or saline injection and assessed for striatal tubulins and DAergic markers.

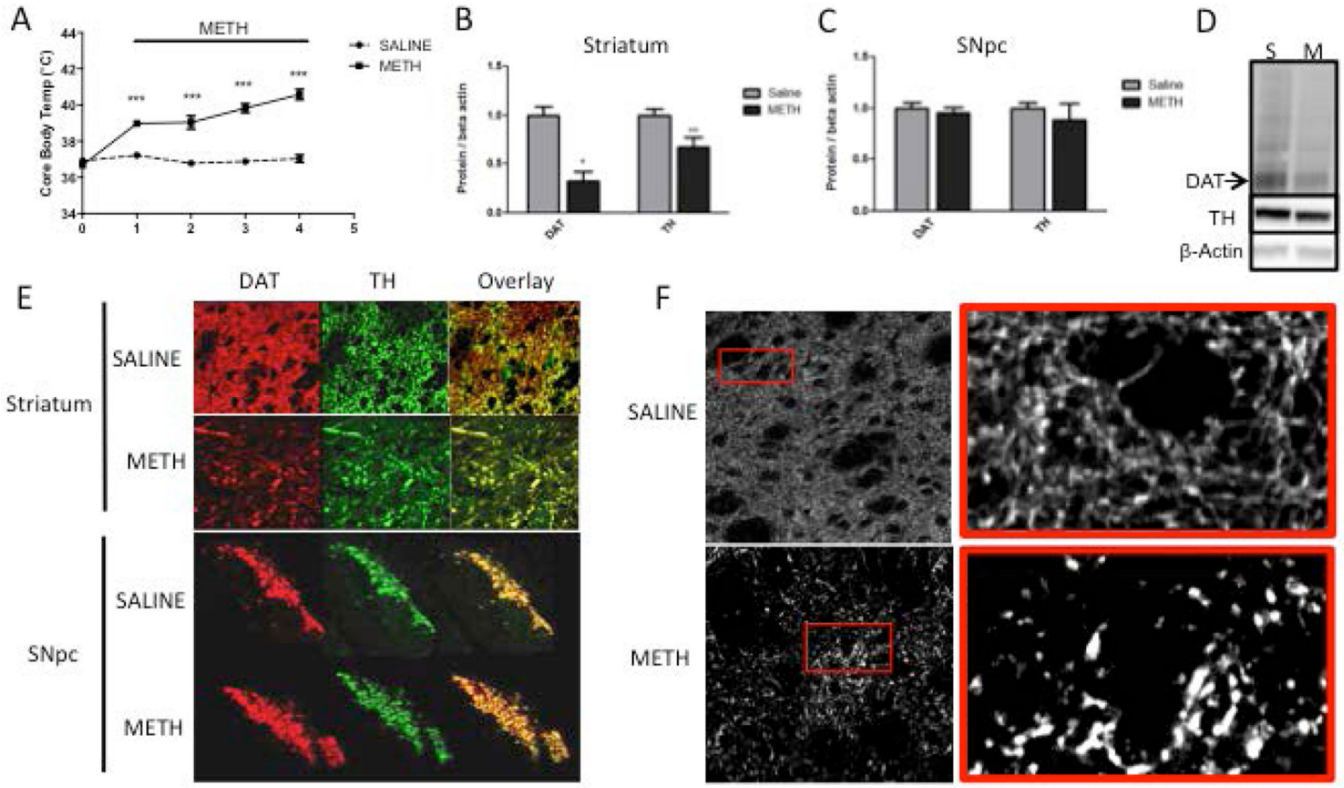

Figure 2. Levels of dopaminergic (DAergic) markers in the rat striatum and substantia nigra *pars compacta* (SNpc) 3 days after binge methamphetamine (METH)

Rats were treated with four successive injections (i.p.) of either saline (SAL) (1 mL/kg) or METH-HCl (10 mg/kg) at 2-h intervals. Three days later, the animals were sacrificed and brain tissue was harvested. (A) Core body temperature of animals during binge METH or SAL treatment measured 1 h after each injection. METH induced significant hyperthermia over time (***p<0.001 SAL vs. METH, two-way ANOVA with repeated measures followed by Student-Newman-Keuls *post hoc* test, n=5). (B, C) Quantified dopamine transporter (DAT) and tyrosine hydroxylase (TH) immunoreactivities in the striatum (B) and SNpc (C). METH significantly reduced DAT (−68%) and TH (−33%) levels in the striatum (*p<0.05, **p<0.01, Student's two-tailed *t*-test, n=5) and not in the SNpc. (D) Representative western blot images of DAT (72 kDa), TH (64 kDa), and β-actin (45 kDa) from rats administered saline (S) and METH (M). β-Actin immunoreactivity was used as a loading control. All band density values were normalized to the saline controls. (E) Fluorescently labeled DAT (red) and TH (green) in brain tissue slices of the striatum and SNpc. The images depicting the striatum are magnified 40× to show individual axons; the SNpc images are magnified 4× to show the total surface of this area. Channel overlay shows co-localization of green and red signal in yellow. (F) High-contrast images of TH immunoreactivity in striatal brain slices show the morphology of TH-labeled striatal axons. All data are expressed as mean ± S.E.M.

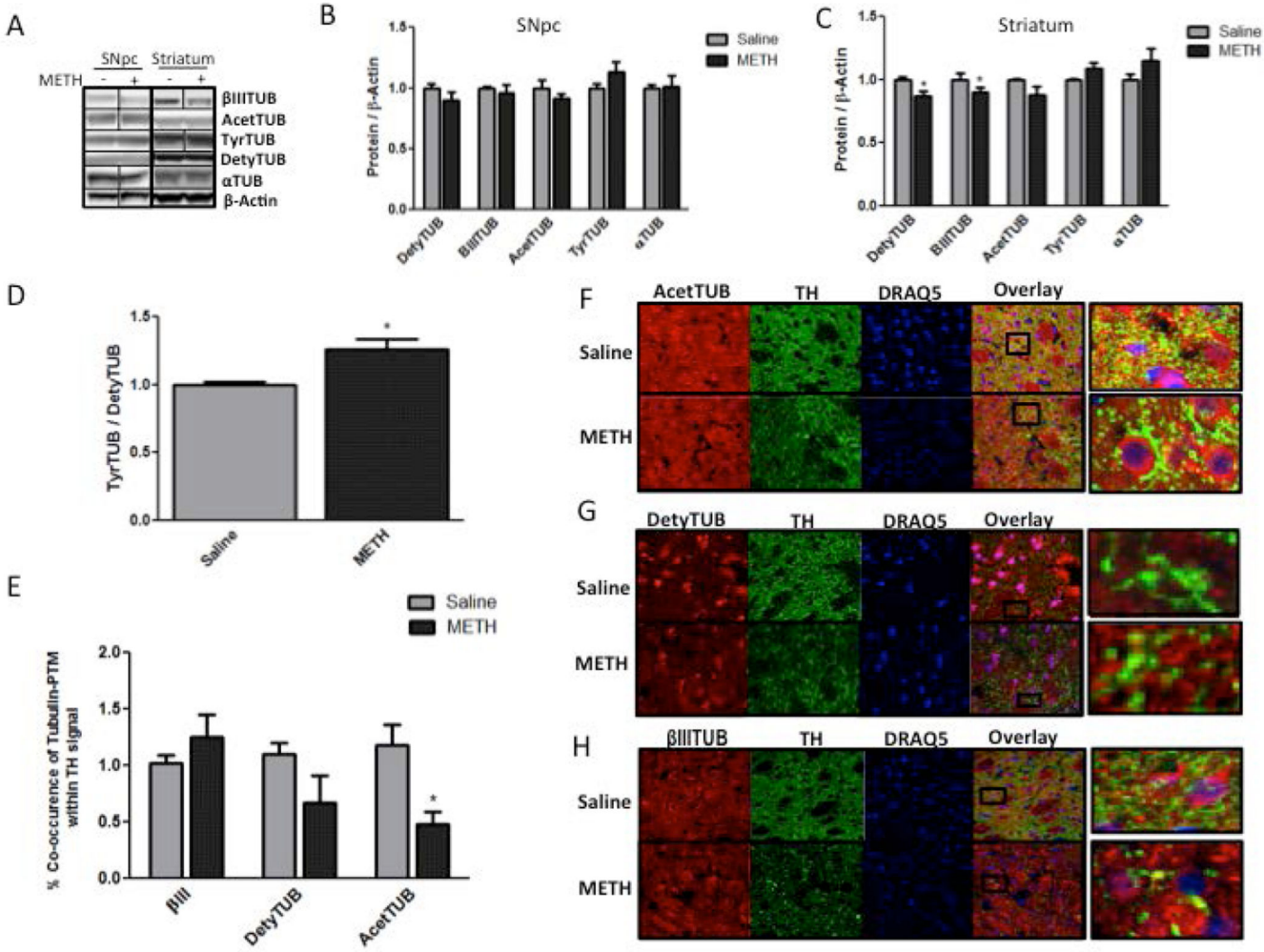

Figure 3. Tubulins in the striatum and substantia nigra *pars compacta* (SNpc) 3 days after methamphetamine (METH) treatment

Rats were treated with four successive injections (i.p.) of either saline (SAL) (1 mL/kg) or METH-HCl (10 mg/kg) at 2-h intervals and sacrificed 3 days later. (A-C) Western blot analysis of lysates from the striatum (B) and SNpc (C) labeled with antibodies specific for detyrosinated α-tubulin (DetyTUB, 50 kDa), tyrosinated α-tubulin (TyrTUB, 50 kDa), βIII tubulin (βIIITUB, 52 kDa), acetylated α-tubulin (AcetTUB, 50 kDa), α-tubulin (αTUB, 50 kDa), and β-actin (45 kDa) (loading control). (A) Representative western blot images for B and C. METH significantly decreased the immunoreactivity of DetyTUB (−14%) and βIIITUB (−10%) in striatal but not nigral tissue lysates (*$p<0.05$ Student's two-tailed *t*-test with Bonferroni correction for multiple comparisons, n=5). (D) The ratio of TyrTUB to DetyTUB was increased in striatal lysates (+26%, *$p<0.05$ Student's two-tailed *t*-test, n=5). (F-H) Images of fixed striatal brain slices fluorescently labeled for (F) AcetTUB, (G) DetyTUB, and (H) βIIITUB (all depicted in red) as well as for tyrosine hydroxylase (TH) (green) and nuclei (blue). (E) Quantification of co-occurrence of tubulins and TH in striatal tissue slices. Co-occurrence is defined as the percentage of TH signal that contains the tubulin signal above a threshold. METH significantly decreased the immunoreactivity of

AcetTUB (−52%) and DetyTUB (−33%) in TH-positive striatal axons (*p<0.05, Student's two-tailed *t*-test with Bonferroni correction n=5). All band density values and co-occurrence values were normalized to the respective saline controls. The data are expressed as mean ± S.E.M. *

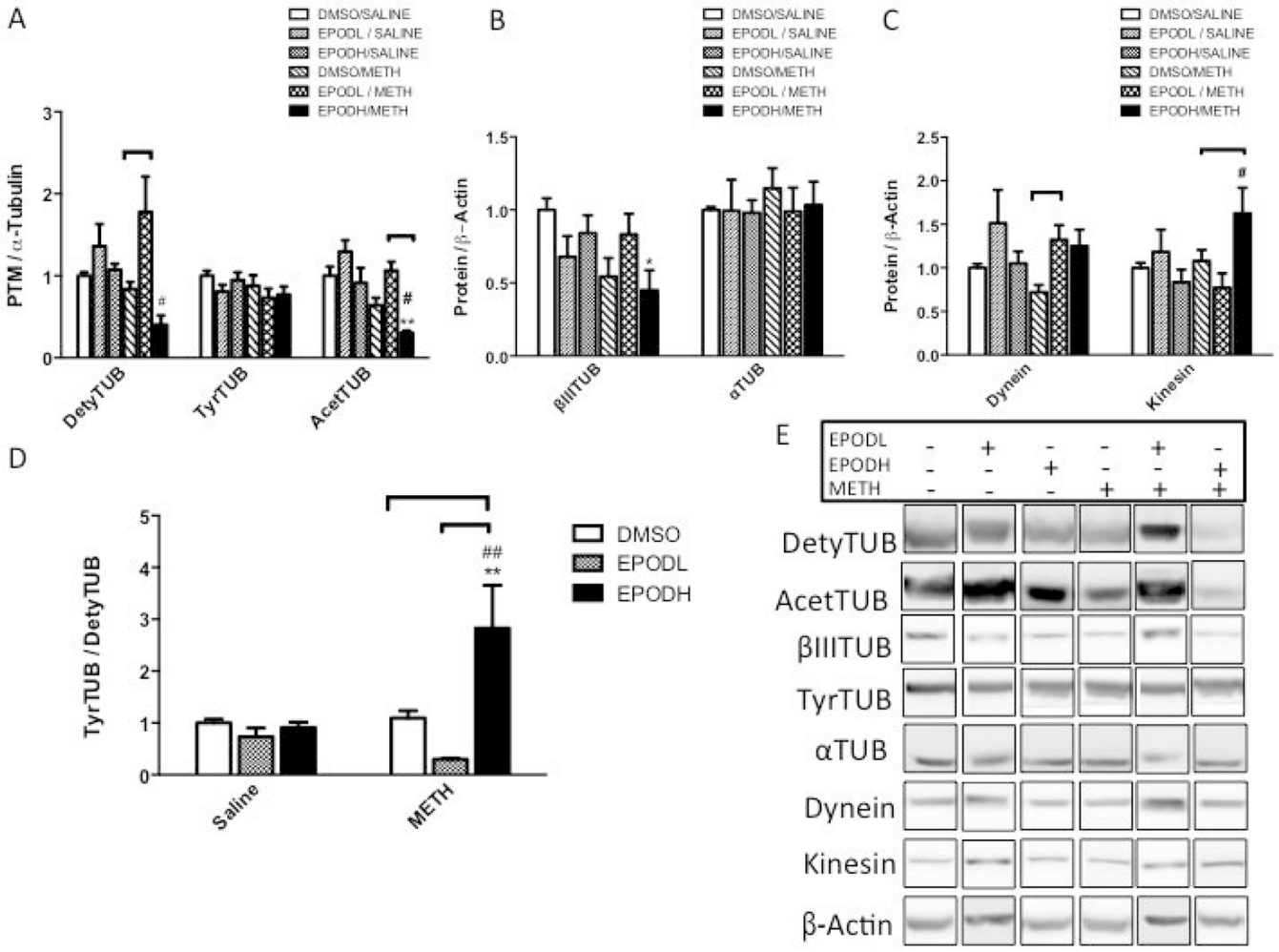

Figure 4. Striatal tubulins in rats treated with epothilone D (EpoD) and methamphetamine (METH)

A group of rats was divided into 6 subgroups. Two subgroups were treated with four successive injections (i.p.) of either saline (SAL) (1 mL/kg) or METH-HCl (10 mg/kg). The remaining subgroups were also treated with a low dose of epothilone (EpoD) (EpoDL; 0.5 mg/kg), high dose of EpoD (EpoDH; 5 mg/kg) or DMSO before, during, and after binge METH or saline. All animals were sacrificed 3 days later and the striatal lysates were analyzed for (A) posttranslational modifications of α-tubulin (α-TUB): detyrosinated α-tubulin (DetyTUB, 50 kDa), tyrosinated α-tubulin (TyrTUB, 50 kDa), and acetylated α-tubulin (AcetTUB 50 kDa) (B) tubulin isoforms: α-TUB (50 kDa) and βIII tubulin (βIIITUB, 52 kDa), and (C) motor proteins: kinesin (heavy chain, 120 kDa) and dynein (95 kDa). α-TUB was used as a loading control for DetyTUB AcetTUB and TyrTUB while β-actin (45 kDa) was used as a loading control for other proteins. The immunoreactivities were normalized to saline/DMSO-treated controls. (A) Compared to METH alone, EpoDL/METH treatment increased whereas EpoDH/METH treatment decreased the immunoreactivity of DetyTUB (+112% and −48%, respectively) and AcetyTUB (+66% and −48%, respectively). The DetyTUB and AcetyTUB in EpoDH/METH rats were also significantly decreased when compared to EpoDH/SAL controls (−62% and 67%, respectively). (B-D) In the EpoDH/

METH-treated rats, βIIITUB immunoreactivity was decreased (−55% *vs.* DMSO/SAL) kinesin immunoreactivity was increased (+95% *vs.* EpoDH/SAL) and the ratio of TyrTUB to DetyTUB was increased (2.8 fold *vs.* DMSO/SAL and EpoDH/SAL). (E) Representative western blot images. All data are expressed as mean ± SEM. *p<0.05, **p<0.01 treatment *vs.* DMSO/SAL, $^{\#}$p<0.05, $^{\#\#}$p<0.01, EpoD/SAL vs. EpoD/METH, ∏ (bracket) p<0.05 differences within SAL and METH subgroups, one-way ANOVA followed by Tukey's *post hoc* test, n=4–13. Analysis of DetyTUB and AcetTUB data by two-way ANOVA with Tukey *post hoc* test revealed co-treatment (DMSO, EpoD) × treatment (SAL, METH) interaction for DetyTUB and TyrTUB/DetyTUB ratio ($F_{(2.42)}$ = 2.82, p<0.05 and $F_{(2,43)}$ = 6.29, p<0.01, respectively).

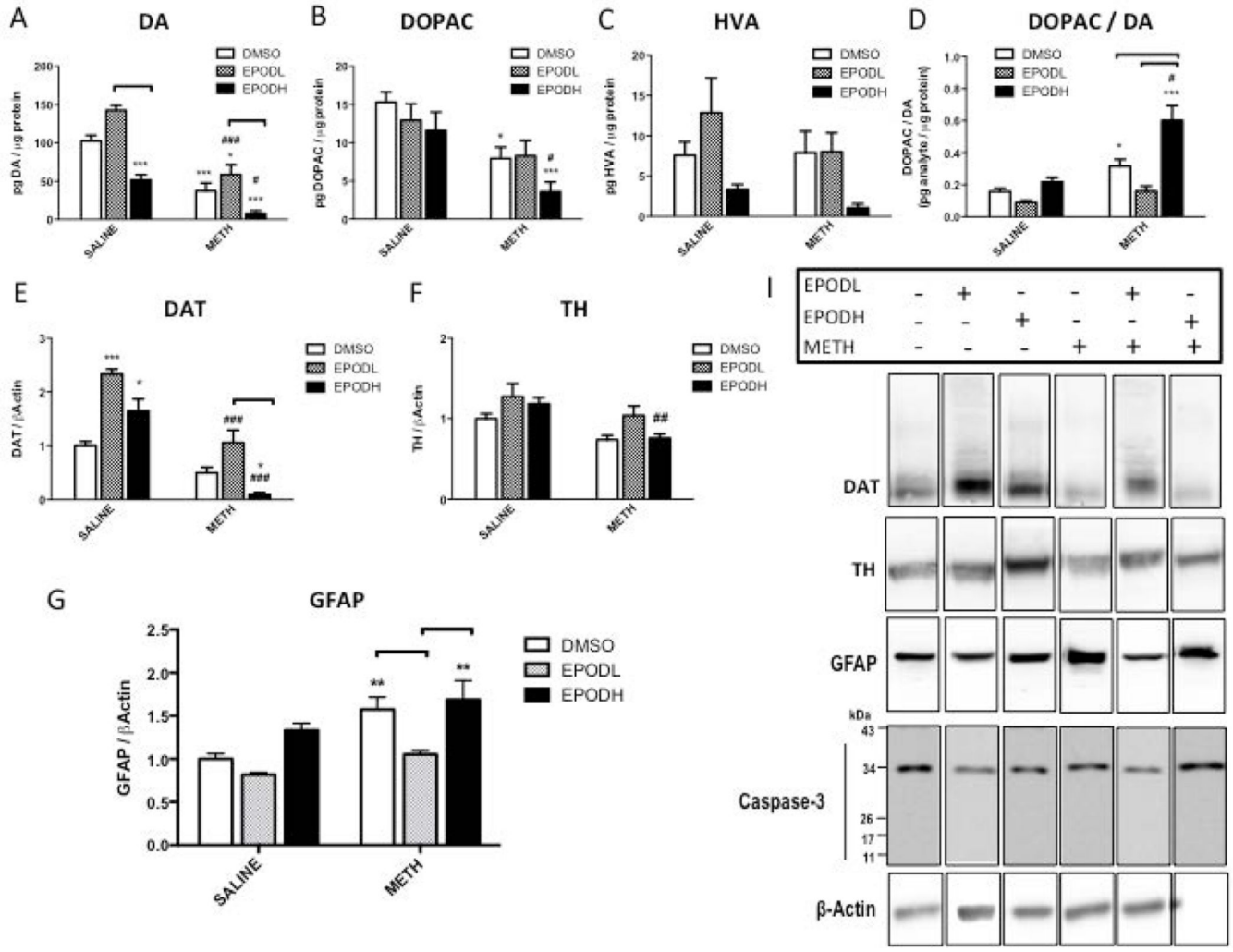

Figure 5. Striatal dopaminergic (DAergic) markers in rats treated with epothilone D (EpoD) and methamphetamine (METH)

A group of rats was divided into 6 subgroups. Two subgroups were treated with four successive injections (i.p.) of either saline (SAL) (1 mL/kg) or METH-HCl (10 mg/kg). The remaining subgroups were also treated with a low dose of epothilone (EpoD) (EpoDL; 0.5 mg/kg), high dose of EpoD (EpoDH; 5 mg/kg) or DMSO before, during, and after binge METH or saline. All animals were sacrificed 3 days later and the striatal lysates were analyzed for (A-F) DAergic markers, glial fibrillary acidic protein (GFAP, 50 kDa) and (I) caspase-3 (35 and 17 kDa). β-Actin was used as a loading control. EpoDL and EpoDH alone increased DAT immunoreactivity (2.3 fold and 1.6 fold, respectively); they have the opposite effects on DA (+44% and −48%, respectively). EpoDH/METH treatment potentiated METH-induced deficits in striatal (A) DA (−63% *vs.* 92%), (B) 3,4-dihydroxyphenylacetic acid (DOPAC) (−48% *vs.* −77%), and (F) dopamine transporter (DAT, 60–80 kDA) (−50% *vs.* −99%) as well as (D) METH-induced increase in DOPAC/DA ratio (+32% *vs.* +60%). Compared to DMSO/SAL, DA and DAT content in EpoDL/METH group was decreased by 63% and 50%, respectively, while compared to EpoDL/SAL these markers were decreased by 59% and 55%, respectively. (F) Tyrosine hydroxylase (TH, 60 kDa) content in EpoDH/

METH group significantly decreased in relation to EpoDH/SAL group (−36%). (G) DMSO/METH and EpoDH/METH treatment increased GFAP immunoreactivity (+57% and +69%, respectively). (I) Neither treatment activated caspase-3. (I) Representative western blot images. Band density values were normalized to DMSO/SAL values. All data are expressed as mean ± SEM. *p<0.05, **p<0.01, ***p<0.001, treatment *vs.* DMSO/SAL, $^{\#}$p<0.05, $^{\#\#}$p<0.01, $^{\#\#\#}$p<0.001, EpoD/SAL vs. EpoD/METH, ∏ (bracket) p<0.05 differences within SAL and METH subgroups, one-way ANOVA followed by Tukey's *post hoc* test, n=4–13. Analysis of DA, DAT and DOPAC/DA data by two-way ANOVA with Tukey *post hoc* test revealed co-treatment (DMSO, EpoD) × treatment (SAL, METH) interaction for DAT and DOPAC/DA ratio ($F_{(2.43)}$ = 7.17, p<0.01 and $F_{(2,44)}$ = 5.79, p<0.01, respectively).

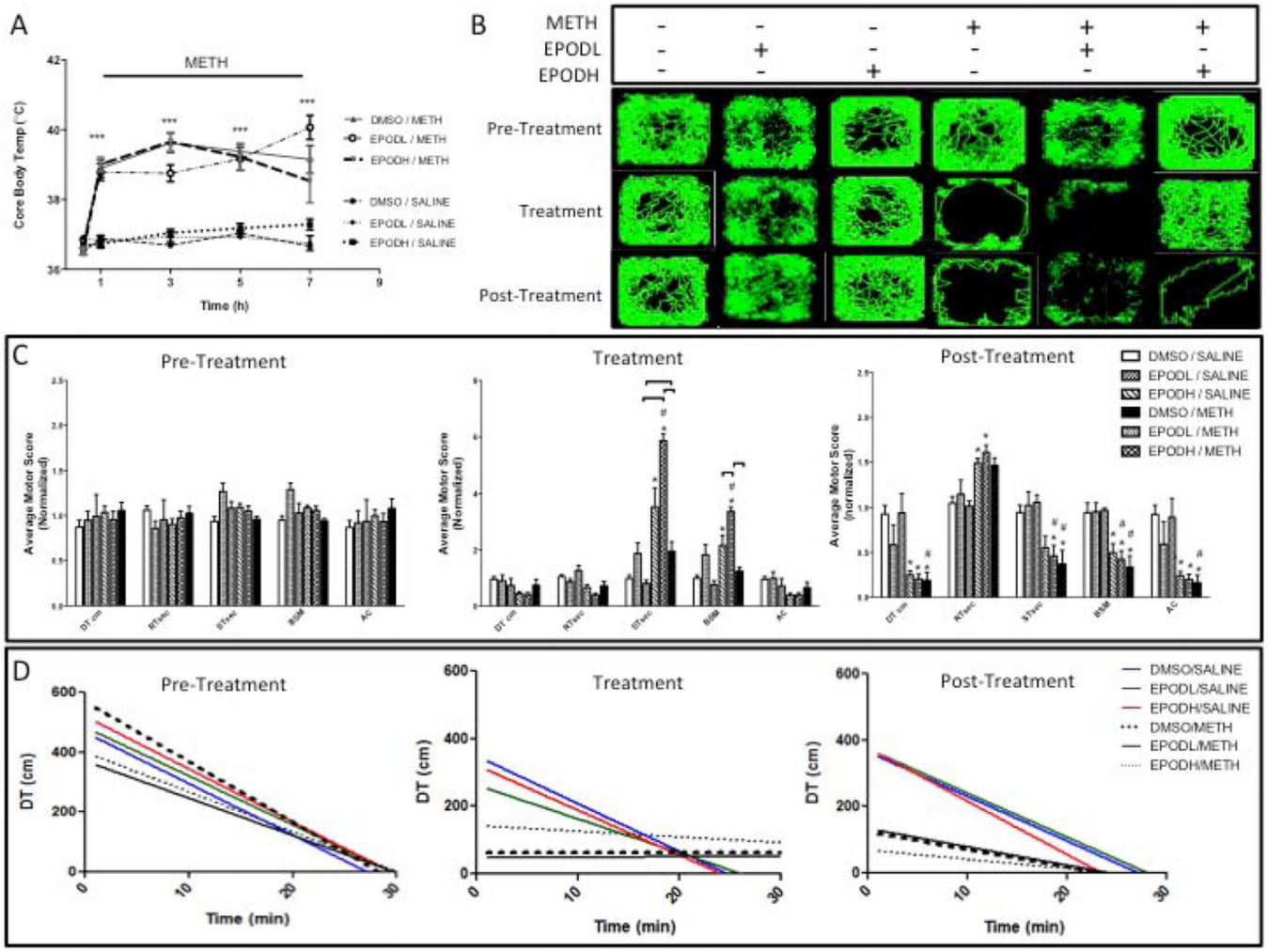

Figure 6. Locomotor activity of rats treated with epothilone D (EpoD) and methamphetamine (METH)

A group of rats was divided into 6 subgroups. Two subgroups were treated with four successive injections (i.p.) of either saline (SAL) (1 mL/kg) or METH-HCl (10 mg/kg). The remaining subgroups were also treated with a low dose of epothilone (EpoD) (EpoDL; 0.5 mg/kg), high dose of EpoD (EpoDH; 5 mg/kg) or DMSO before, during, and after binge METH or saline. (A) Core body temperatures were recorded before METH (0 h) and 1 h after each METH or SAL injection. METH induced significant hyperthermia over time (***p<0.001 SAL vs. METH, two-way ANOVA with repeated measures followed by Student-Newman-Keuls *post hoc* test, n=3–11). (B) Representative activity maps. Continuous green line traces animal's movement during each 30-min session. The animals treated with EpoDH/METH displayed less stereotypy (seen as dense green nodules) than other METH groups; instead, they maintained hyperlocomotion during METH administration. (C) Quantification of total motor activity counts during the 30-min open-field tests performed 24 h before METH (pre-treatment), after the third METH injection (treatment), and 24 h after the last METH injection (post-treatment). The rats treated with EpoDL/SAL displayed increased stereotypy during the treatment phase. The animals treated with DMSO/METH also displayed more stereotypy than DMSO/saline controls but less than

EpoDL/METH-treated rats. (D) Acclimation behavior during each of the 30-min locomotor activity sessions. Linear regression analysis was performed between the distance traveled and time. All data are expressed as mean ± SEM. *p<0.05, treatment *vs.* DMSO/SAL, #p<0.05, EpoD/SAL vs. EpoD/METH, ∏ (bracket) p<0.05 differences within SAL and METH subgroups, one-way ANOVA followed by Tukey's *post hoc* test, n=4–13. Analysis of stereotypy data by two-way ANOVA with Tukey *post hoc* test revealed a trend for co-treatment (DMSO, EpoD) × treatment (SAL, METH) interaction for total time spent in stereotypy (ST) ($F_{(2,36)}$ = 7.17, p=0.073). Abbreviations: DT, total distance traveled; RT, total time at rest; ST, total time spent in stereotypy; AT, total ambulatory time; BSM, burst of stereotypy; HC, horizontal counts; AC, ambulatory counts; EpoDL, low-dose EpoD; EpoDH, high-dose EpoD.